

Impaired nociception in the diabetic *Ins2*^{+/Akita} mouse

Nisha Vastani^{1*}, Franziska Guenther^{1,2*}, Clive Gentry¹, Amazon L. Austin³,
Aileen J. King³, Stuart Bevan¹ and David A. Andersson^{1†}

Addresses: ¹Wolfson Centre for Age-Related Diseases, King's College London, London SE1 1UL, United Kingdom;

²Institut für Physiologie & Pathophysiologie, Universität Erlangen-Nürnberg, Universitätsstraße 17, D-91054 Erlangen, Germany;

³Diabetes & Nutritional Sciences Division, King's College London, London SE1 1UL, United Kingdom

*Joint first authors

†**Corresponding author:** David A. Andersson

Wolfson CARD, Hodgkin Building, Guy's Campus, King's College London, London SE1 1UL, United Kingdom

Email: david.andersson@kcl.ac.uk

Tel: +44 2078486141

Running title: Sensory neuropathy in the *Ins2*^{+/Akita} mouse

Abstract

The mechanisms responsible for painful and insensate diabetic neuropathy are not completely understood. Here, we have investigated sensory neuropathy in the *Ins2^{+/Akita}* mouse, a hereditary model of diabetes. Akita mice become diabetic soon after weaning, and we show that this is accompanied by an impaired mechanical and thermal nociception and a significant loss of intraepidermal nerve fibers. Electrophysiological investigations of skin-nerve preparations identified a reduced rate of action potential discharge in *Ins2^{+/Akita}* mechanonociceptors compared to wildtype littermates, whereas the function of low threshold A-fibers was essentially intact. Studies of isolated sensory neurons demonstrated a markedly reduced heat responsiveness in *Ins2^{+/Akita}* DRG neurons, but a mostly unchanged function of cold sensitive neurons. Restoration of normal glucose control by islet transplantation produced a rapid recovery of nociception, which occurred before normoglycemia had been achieved. Islet transplantation also restored *Ins2^{+/Akita}* intraepidermal nerve fiber density to the same level as wildtype mice, indicating that restored insulin production can reverse both sensory and anatomical abnormalities of diabetic neuropathy in mice. The reduced rate of action potential discharge in nociceptive fibers and the impaired heat responsiveness of *Ins2^{+/Akita}* DRG neurons suggests that ionic sensory transduction and transmission mechanisms are modified by diabetes.

Introduction

Diabetic sensory neuropathy is a major cause of chronic pain and paraesthesias, but the most common symptom is sensory loss, and insensate neuropathy is a dominant risk factor for foot ulcers and amputations (1–3). Rodent models of diabetic neuropathy recapitulate many anatomical and sensory abnormalities observed in patients, and thus appear suitable for translational mechanistic studies (4,5). The sensory abnormalities reported from different rodent models differ qualitatively, with diabetic rats commonly displaying tactile and thermal hypersensitivity, whereas mice usually exhibit loss of sensitivity to mechanical or thermal stimulation similar to that seen in patients (3–5).

Patients with diabetic neuropathy typically display a reduced tactile sensitivity and a reduced ability to detect skin cooling and heating (6–8). A compromised ability to detect stimulation with von Frey filaments and to sense vibration are thus important and simple diagnostic tools for early signs of diabetic neuropathy (9,10). In addition to the loss of sensation and development of pain and paraesthesias, diabetic neuropathy is characterized by reduced nerve conduction velocity, distal fiber loss and reduced axon diameters (11,12). The relative importance of abnormalities in sensory transduction, conduction and anatomical structure for painful or insensate neuropathy *in vivo* is currently unclear, but the presence of sensory abnormalities cannot be used to discriminate between patients with painless and painful diabetic neuropathy (12).

Here, we present a detailed characterization of sensory neuropathy in the *Ins2*^{+/*Akita*} mouse using behavioral, cellular and neurophysiological approaches. Mice that are heterozygous for the *Ins2*^{C96Y} (*Ins2*^{+/*Akita*}) mutation develop β -cell endoplasmic reticulum-stress, produce little insulin and become diabetic soon after weaning (13,14). The phenotype is more

serious in male than female mice (13,14). Since the *Ins2*^{C96Y} mutation leads to spontaneous development of diabetes, the Akita strain provides a convenient translational model suitable for investigations of diabetic complications and islet transplantations (15). Relatively little information is available about the sensory phenotype of *Ins2*^{+/*Akita*} mice, whereas autonomic neuropathy has been examined in more detail previously (16). The results reported here show that *Ins2*^{+/*Akita*} mice rapidly develop impaired mechanosensation following the onset of hyperglycemia, later followed by impaired thermal (hot and cold) nociception. Investigations of skin-saphenous nerve preparations demonstrate a reduced rate of action potential discharge in mechanosensitive A- and C-nociceptors at high stimulus intensities. The reduced behavioral sensitivity to noxious heat was associated with a reduced proportion of heat-sensitive DRG neurons in *Ins2*^{+/*Akita*} mice, as well as a reduced $[Ca^{2+}]_i$ -response amplitude in heat sensitive neurons.

Materials and methods

Mice and behavioral tests

Behavioral experiments were carried out according to the U.K. Home Office Animal Procedures (1986) Act. All procedures were approved by the King's College London Animal Welfare and Ethical Review Body and conducted under the UK Home Office Project License PPL 70/7510. *Ins2*^{+/*Akita*} mice were obtained from The Jackson Laboratory (Maine USA, JAX stock #003548, MGI: 1857572) and maintained on the C57Bl/6J strain. Blood glucose was monitored routinely by Contour XT blood glucose meter (Bayer Healthcare, UK) or Stat Strip Xpress meter and strips (Nova Biomedical, UK).

The Randall-Selitto paw-pressure test was performed using an Analgesymeter (Ugo-Basile, Italy). Mice were kept in their holding cages to acclimatize (10–15 min) to the experimental room. The experimenter lightly restrained the mouse and applied a constantly increasing pressure stimulus to the dorsal surface of the hind paw using a blunt conical probe. The nociceptive threshold was defined as the force in grams at which the mouse withdrew its paw. A force cut-off value of 150 g was used to avoid tissue injury.

Tactile sensitivity was assessed using von Frey filaments (0.008-2 g) according to Chaplan's up-down method (17). Animals were placed in a Perspex chamber with a metal grid floor allowing access to their plantar surface and allowed to acclimatize prior to the start of the experiment. The von Frey hairs were applied to the plantar surface of the hind paw with enough force to allow the filament to bend, and held static for approximately 2-3 s. The stimulus was repeated up to 5 times at intervals of several seconds. The stimulus interval was adapted to allow for the resolution of any behavioral responses to previous stimuli. A positive response was noted if the paw was sharply withdrawn or if the mouse flinched upon removal of the hair. Any movement of the mouse, such as walking or grooming, was deemed an unclear response, and in such cases the stimulus was repeated. If no response was noted a higher force hair was tested and the filament producing a positive response recorded as the threshold.

Thermal nociception was examined by lightly restraining the animal and placing one of the hind paws onto a cold- or hot-plate maintained at 10°C or 50°C (18,19). The paw withdrawal or escape latency was measured using 30 s as a cut-off to avoid tissue injury.

Skin-nerve preparations

Single fiber recordings were carried out from 18-20 week old adult male littermate *Ins2^{+/+}* and *Ins2^{+/Akita}* mice. The saphenous nerve and hind-paw hairy skin were dissected free and immediately placed in warm (32°C) oxygenated synthetic interstitial fluid (SIF) containing (in mM); 108 NaCl, 3.5 KCl, 0.7 MgSO₄, 26.2 NaHCO₃, 1.65 NaH₂PO₄, 9.6 Na-gluconate, 5.55 glucose, 1.53 CaCl₂, buffered to pH 7.4 by bubbling carbogen (95% O₂ and 5% CO₂). The skin was pinned down, corium side up and the saphenous nerve was placed on a mirrored platform covered in paraffin oil in a separate chamber containing a SIF-paraffin oil interface. The nerve was desheathed and teased into thin filaments, which were placed onto a gold electrode. Electrical signals were recorded using the DAM80 differential amplifier (World Precision Instruments), band-pass filtered at 300 Hz and 10 kHz and digitized and stored on a computer using the Micro1401 data acquisition unit and SPIKE2, version 8 software (Cambridge Electronic Design). Action potentials were also visualized using an oscilloscope (Gould, 420 series).

Receptive fields of mechanosensitive primary afferents located in the hairy skin of the hind paw and lower hind limb were identified using a blunt glass rod and thereafter stimulated with brief electrical pulses (1ms, Digitimer, DS2) to determine the fiber's conduction velocity. Fibers with conduction velocity below 1.2m/s were classified as C fibers, those between 1.2 and 10m/s as A δ fibers and those with conduction velocity exceeding 10m/s as A β fibers (20).

The mechanical threshold of single fibers was assessed by identifying the minimum force (delivered as a 2s step, by a computer-driven, feedback-controlled stimulator) required to evoke 2 action potentials (21). Adaptation properties were characterized by applying 15s sustained mechanical force 0.5, 1, 2, 4, 5, 10, 15 and 20g with 2 min inter-stimulus intervals

to reduce tachyphylaxis. The encoding properties of mechano-sensitive A δ and C fibers were examined by applying ramp shaped mechanical stimuli.

The thermal sensitivity of some C fibers was investigated. A metal ring was used to isolate the receptive field and a 60 second cold stimulus ~ 31 to 4°C was applied by superfusing pre-cooled SIF. Thereafter, a 20 second heat stimulus of ~ 32 to 48°C was applied by pre-warming the SIF through a heated-element. The rate of temperature increase was determined using a custom-made feedback-controlled device. For both the cold and heat stimuli, peristaltic pumps were used to control the SIF flow rate. A digital temperature probe was placed inside the ring to record the temperature (Greisinger, GIA 2000) at the skin. A thermally elicited response was considered if a minimum of two action potentials occurred and the temperature at which the second action potential fired was recorded as the thermal threshold.

Data were analyzed offline using the SPIKE2 software (Cambridge Electronic Design). Action potentials were discriminated using templates based on their amplitude and waveform.

DRG neurons

DRG neurons were dissociated enzymatically (using collagenase and trypsin) from ganglia dissected from 12 (1 of each phenotype) or 20 weeks old (2-3 of each genotype) male littermate *Ins2^{+/+}* and *Ins2^{+/Akita}* mice using methods described previously (22). Isolated neurons were plated on poly-d-lysine coated coverslips and maintained at 37°C in 95% air, 5% CO_2 . Wildtype (*Ins2^{+/+}*) neurons were maintained in MEM AQ containing 5.6 mM glucose (Sigma, Poole, UK) and *Ins2^{+/Akita}* neurons in DMEM glutamax containing 25 mM glucose (Thermofisher, UK), each supplemented with 10 % fetal bovine serum, 100 U/ml penicillin, 100 $\mu\text{g}/\text{ml}$ streptomycin, 10 μM cytosine arabinoside and 50 ng/ml NGF (Promega,

Southampton, UK) for up to 24 hours before experimentation. The serum content of insulin makes the final concentration in medium 4pM, a concentration far below that required to support trophic effects on isolated DRG neurons (23).

Intracellular $[Ca^{2+}]_i$ -measurements

DRG neurons were loaded with 2.5 μ M fura-2 AM (Invitrogen) in the presence of 1 mM probenecid and 0.01% pluronic acid for approximately one hour at 37°C. In all experiments the cells were constantly superfused with physiological saline solution containing (in mM) 140 NaCl, 5KCl, 10 Glucose, 10 HEPES, 2 $CaCl_2$ and 1 $MgCl_2$, pH 7.4 (NaOH). Fura-2 was excited at wavelengths of 340 and 380 nm and light emission measured at wavelengths >520nm. Solutions were applied through a tube placed in close proximity of the cells and ratio images were captured every 2 s. Data were analysed using ImageMaster software (PTI, New Jersey, USA) to obtain emission intensity ratios ($R_{(340/380)}$) in individual cells.

Intraepidermal nerve fibers

Hind paw skin was dissected and fixed in 4 % paraformaldehyde (PFA) in phosphate-buffered saline and kept at room temperature until embedded in paraffin wax. 8 μ m thick sections were cut and stained with rabbit polyclonal anti-PGP9.5 (Ultraclone Ltd, UK) overnight at 4 °C. Staining was visualized using a biotinylated goat anti-rabbit IgG (Vectorlabs), followed by streptavidin-Alexa 568 (Invitrogen). Skin sections were additionally stained with DAPI to visualize nuclei. The high density of nuclei in the epidermis provides a clear indication of the location of the basement membrane. We have adapted the general method described for human tissue (24,25) to suit thin sections prepared from mouse skin (26,27). The number of intraepidermal nerve fibers extending intact from the basement

membrane per mm was quantified using a Zeiss Apotome microscope. The observer was blinded to the identity of the animal.

Islet isolation and transplantation

Islets were isolated from 10-12 week old C57Bl/6J mice (Charles River, UK) using collagenase digestion (1mg/ml, type XI, Sigma Aldrich, UK) and density gradient separation (Histopaque-1077, Sigma Aldrich, UK) as previously described (28). Islets were washed in culture medium (RPMI-1640 supplemented with 10% Foetal Bovine Serum and 1% Penicillin/Streptomycin) and divided into groups of 500 for same day transplantation.

Male 14-20 week old $Ins2^{+/Akita}$ mice were transplanted with 500 freshly isolated islets into the renal subcapsular space. Mice were anaesthetized with 1–5% isoflurane and 95% oxygen (1l/min). The kidney was exposed by a lumbar incision and a small perforation in the kidney capsule was made using a 23G needle. Islets were pelleted in PE50 tubing before being injected under the renal capsule using a Hamilton syringe (Hamilton, USA). The capsule was then cauterized and the mouse peritoneum and skin were sutured. Mice were given carprofen (Caprieve, 4mg/kg; s.c.; Norbrook, UK) and bupivacaine (Marcaine 0.5% solution, 2mg/kg, s.c., Aspen Medical, UK) for post-operative analgesia.

Data analysis

Quantitative data are presented as the individual raw data points or mean \pm SEM, and the number of observations (animals or cells indicated by n). Data were analyzed by t-test, Mann-Whitney U-test or ANOVA followed by Tukey's *post-hoc* test as appropriate. Categorical data were analyzed by Fisher's exact test. Boxplots show the median, interquartile range, with whiskers indicating the 5th and 95th percentile. Statistical analysis

was performed using Statistica or IBM SPSS (version 20 or higher). Differences were considered significant at $p < 0.05$.

Drugs and Chemicals

Icilin was purchased from Tocris (Bristol, UK), salts and all other reagents from Sigma-Aldrich (Gillingham, UK), unless stated otherwise.

Results

Diabetes in $Ins2^{+/Akita}$

$Ins2^{+/Akita}$ mice developed hyperglycemia soon after weaning and became diabetic around 4-5 weeks of age (Fig. 1A). Hyperglycemia progressively worsened in male $Ins2^{+/Akita}$ mice, and around 12 weeks of age, their blood glucose values reached or exceeded the upper limit of most blood glucose meters (~33 mM). In contrast, blood glucose peaked around 6 weeks of age in female $Ins2^{+/Akita}$ mice, and thereafter declined towards normoglycaemia. Male, but not female $Ins2^{+/Akita}$ mice gained body weight at a reduced rate compared to wildtype littermates (Fig. 1B).

Nociception in the $Ins2^{+/Akita}$ mouse

We assessed the behavioral sensitivity of male and female, wildtype and $Ins2^{+/Akita}$ mice to noxious mechanical and thermal stimulation, starting soon after weaning and continuing until ~20 weeks of age. Mechanical nociception was assessed using the Randall-Selitto paw pressure test and punctate stimulation with von Frey filaments, and the sensitivity to noxious thermal stimulation was determined using a modified cold- and hot-plate assay (18,19). Both male and female $Ins2^{+/Akita}$ mice developed a reduced sensitivity in the paw-pressure test, almost immediately after the onset of hyperglycemia (Fig. 1C). Furthermore,

female *Ins2^{+/Akita}* mice progressively recovered from mechanical insensitivity from about 10-12 weeks, when their blood glucose concentration started to decline. From 14 weeks of age, female *Ins2^{+/Akita}* mice were no longer distinguishable from wildtype littermates in the paw-pressure test, suggesting that the glycemic profile has a dynamic influence on mechanical nociception in mice (Fig. 1C). The paw withdrawal threshold in response to stimulation with calibrated von Frey filaments did not differ between *Ins2^{+/Akita}* and wildtype littermates, apart from a transiently reduced sensitivity in male *Ins2^{+/Akita}* mice around 10 weeks of age (Fig. 1D).

The paw withdrawal latency of male *Ins2^{+/Akita}* mice in the cold (10°C) and hot (50°C) plate tests increased at around 9-10 weeks of age and thereafter remained elevated until at least 19-20 weeks of age (Fig. 1e, f). In contrast, female *Ins2^{+/Akita}* mice remained indistinguishable from wildtype mice in both thermal tests, apart from a transiently reduced cold sensitivity around 10 weeks of age (Fig. 1 e, f). The paw-pressure thus appears to be a particularly sensitive parameter for assessing sensory abnormalities in diabetic mice, and our results indicate that the degree of hyperglycemia experienced by female *Ins2^{+/Akita}* mice is not sufficient to influence the behavioral sensitivity to noxious hot or cold stimulation.

Low-threshold mechanoreceptors

The conduction velocities and the mechanical response thresholds of rapidly adapting (RA), slowly adapting (SA) A β and A δ down hair (DH) fibers were unchanged in preparations from 18-20 weeks old male diabetic *Ins2^{+/Akita}* mice compared to fibers in age-matched male WT littermates (table 1). Furthermore, RA and DH fibers from diabetic *Ins2^{+/Akita}* mice displayed an unchanged action potential firing pattern to sustained force across the range of forces tested (0.5-20g) compared to fibers in preparations from wildtype littermates (Fig. 2A, B, E,

F). We did note a significantly reduced firing rate in *Ins2^{+/Akita}* SA fibers in response to the lowest force (0.5g, $p=0.01$, Mann-Whitney *U*-test, Fig 2C). This observation suggests that SA fibers in *Ins2^{+/Akita}* mice display an accelerated adaptation at low stimulus strengths, compared to WT mice (Fig 2D).

A δ - and C-mechanoreceptors

The conduction velocities of *Ins2^{+/Akita}* nociceptive A δ -mechanoreceptors (AM, (29)) were unchanged compared to WT fibers in preparations from 20 week old male mice. Unmyelinated C-mechanoreceptors (CM, (30)) from *Ins2^{+/Akita}* however displayed a reduced conduction velocity compared to WT fibers ($p=0.007$, Mann-Whitney *U*-test, Table 1), as previously noted in diabetic rats (31). The response threshold in AM fibers from diabetic mice was modestly increased (Table 1), but the most striking differences between the response properties of nociceptors from *Ins2^{+/Akita}* and wildtype mice were revealed by suprathreshold stimulation. Wildtype AM fibers faithfully encoded mechanical force with a linear increase in discharge rate. In contrast, fibers from *Ins2^{+/Akita}* mice failed to encode stimuli exceeding 10g (Fig. 3A) and displayed a significantly reduced impulse rate in response to the highest mechanical forces (Fig 3A, D). The temporal response profiles evoked by force steps, demonstrates that *Ins2^{+/Akita}* AM fibers failed to reach the maximal, initial impulse rate typical of WT fibers (Fig 3B, C). The mechanical encoding properties of AMs were examined further using ramp-shaped stimuli. Diabetic AM fibers displayed a marginally (but not significantly) reduced average firing frequencies throughout the range of ramp forces used (Fig. 3E, F), an observation which may be consistent with a failure to achieve the initial peak firing rate (Fig. 3C), but a retained ability to encode force in response to continuously increasing ramp stimulation.

Stimulation with force steps produced similar impulse discharge rates in CM fibers from wildtype and *Ins2^{+/Akita}* mice (Fig 4A, B), but responses to the maximal ramp force was significantly reduced in *Ins2^{+/Akita}* CM fibers (Fig. 4C). Although *Ins2^{+/Akita}* CM fibers encoded the intensity of a ramp force stimulus, they appeared to do so at somewhat lower rate than CM fibers in wildtype preparations (Fig. 4D, E).

Heat and cold sensitivity of Ins2^{+/Akita} C-mechanoreceptors

Since diabetic mice displayed behavioral insensitivity to noxious heat and cold, we investigated whether the thermal sensitivity of C-mechanoreceptors was altered in *Ins2^{+/Akita}* mice. The proportion of C-fiber nociceptors that responded to cold (WT; 48%, n=14/29 vs *Ins2^{+/Akita}*; 48%, n=12/25, p=0.98, Pearson's Chi-Squared test) or heat (WT; 51%, n=15/29 vs *Ins2^{+/Akita}*; 45%, n=9/20, p=0.64, Pearson's Chi-squared test) was unchanged in *Ins2^{+/Akita}* compared to WT littermates. Cold sensitive nociceptors (CMC fibers) from diabetic mice exhibited a marginally, but not significantly, reduced temperature threshold for activation (*Ins2^{+/Akita}* 18.2 ± 2°C; WT 21.4 ± 1.7°C, p=0.25, Mann-Whitney *U*-test, Fig. 5 AB). Cold stimulation evoked a significantly reduced number of action potentials in CMC fibers from *Ins2^{+/Akita}* compared to WT mice (*Ins2^{+/Akita}* 18 ± 4; WT 37 ± 7 action potentials, respectively, p=0.018, Mann-Whitney *U*-test, Fig. 5 C-E). Similarly, heat sensitive nociceptors (CMH fibers) from diabetic mice displayed slightly, but not significantly, higher thresholds for heat activation (*Ins2^{+/Akita}* 40.4 ± 1.2°C; WT 38.4 ± 1.0°C, p=0.14, Mann-Whitney *U*-test, Fig. 5 FG) and a reduced number of action potentials in CMH fibers from *Ins2^{+/Akita}* compared to WT (*Ins2^{+/Akita}*; 16 ± 5; WT 25 ± 5 action potentials, respectively, p=0.18, Mann-Whitney *U*-test, Fig. 5 H-J).

Heat and cold sensitivity of $Ins2^{+/Akita}$ DRG neurons

We used $[Ca^{2+}]_i$ -imaging to determine whether the behavioral insensitivity of $Ins2^{+/Akita}$ mice to noxious heat and cold was associated with a compromised thermal sensitivity of isolated DRG neurons (Fig. 6A, B). These experiments were performed on neurons isolated from 12 or 20 weeks old male wildtype and $Ins2^{+/Akita}$ mice. Stimulation with heat ramps (from 25 to 48°C) evoked $[Ca^{2+}]_i$ -responses in a significantly reduced proportion of DRG neurons from $Ins2^{+/Akita}$ mice compared to neurons isolated from wildtype mice ($Ins2^{+/Akita}$ 19.3% 428 of 2222, n=4 animals; wildtype mice 28.5%, 300 of 1054, n=3 animals, Fisher's exact test $P<0.001$). Our measurements revealed a modestly, but significantly, reduced temperature threshold for heat activation in neurons from diabetic mice ($Ins2^{+/Akita}$ $41.5 \pm 0.2^\circ\text{C}$; wildtype $42.9 \pm 0.2^\circ\text{C}$, Fig. 6C; t-test, $P<0.001$). The heat-evoked $[Ca^{2+}]_i$ -response amplitude was reduced by 40% in neurons from $Ins2^{+/Akita}$ mice compared to wildtype ($Ins2^{+/Akita}$ 0.77 ± 0.02 $R_{(340/380)}$; wildtype mice 1.2 ± 0.04 $R_{(340/380)}$; Fig. 6D; t-test, $P<0.001$). These results strongly suggest that an impaired neuronal transduction of noxious heat may contribute to the behavioral insensitivity observed *in vivo*. The proportion of neurons responding to the TRPV1 agonist 1 μM capsaicin ($Ins2^{+/Akita}$ 44.3%, 759 of 1715 neurons, wildtype 42.4%, 447 of 1054, $P>0.3$, Fisher's exact test) and the response amplitude evoked by capsaicin were indistinguishable in cultures from wildtype and $Ins2^{+/Akita}$ mice, indicating that the reduced heat responsiveness of $Ins2^{+/Akita}$ DRG neurons is not likely due to an altered expression of the noxious heat transducer TRPV1.

In contrast to the reduced heat sensitivity of $Ins2^{+/Akita}$ DRG neurons, cold ramps (35-10°C) elicited indistinguishable $[Ca^{2+}]_i$ -responses in neurons isolated from mice of the two genotypes. Cooling stimulated $[Ca^{2+}]_i$ -responses in a small proportion of DRG neurons from 20 weeks old $Ins2^{+/Akita}$ (2.4%, 55 of 2318) and wildtype littermates (2.5 %, 40 of 1604).

Cold-evoked $[Ca^{2+}]_i$ -response amplitudes did not differ between neurons of the two genotypes (Fig. 6F), whereas the cold activation temperature was marginally, but significantly, higher in *Ins2^{+/Akita}* neurons (24.5 ± 0.7 °C) compared to wildtype neurons (22.3 ± 0.9 °C; Fig. 6E). These results indicate that the behavioral insensitivity to noxious cold observed in diabetic *Ins2^{+/Akita}* mice is not associated with compromised cellular cold transduction mechanisms.

*Reduced cutaneous innervation in diabetic *Ins2^{+/Akita}* mice*

Diabetic neuropathy is accompanied by a loss of intraepidermal nerve fibers (IENFs) in patients and in animal models of diabetes, a feature which is frequently used as a diagnostic tool in various small fiber neuropathies (25,32,33). Plantar skin sections prepared from male 20 weeks old diabetic *Ins2^{+/Akita}* mice and wildtype littermates were immunohistochemically labelled for expression of the pan-neuronal marker PGP9.5 (Fig. 7A). We measured the IENF density by counting the number of nerve fibers (mm^{-1}) that extended intact from the epidermal/dermal junction into the epidermis, in thin (8 μm) paraformaldehyde-fixed paraffin-embedded sections of plantar skin (24,25,32). Our results revealed a significant loss of IENFs in diabetic mice. Compared to paw skin from wildtype littermates, the density of PGP9.5-positive epidermal fibers was reduced by about a third in diabetic *Ins2^{+/Akita}* mice (Fig. 7B).

Islet transplantation rapidly reversed symptoms of sensory neuropathy

Finally, we examined whether the impaired nociception and loss of intraepidermal nerve fibers in *Ins2^{+/Akita}* mice could be reversed by improved glycemic control. A group of diabetic *Ins2^{+/Akita}* mice underwent transplantation of pancreatic islets obtained from healthy C57Bl/6J mice (500 islets under the kidney capsule). Following transplantation, blood

glucose declined steadily during the first few days after transplantation, followed by a slower phase of decline and at 3 weeks after islet implantation all mice had glucose levels <15mM (Fig. 7C). Intriguingly, nociception improved rapidly and significantly following transplantation (Fig. 7DE). The behavioral sensitivity to noxious mechanical and cold stimulation recovered to the same level as in naïve wildtype mice within a few days of transplantation, and thus occurred before normoglycemia was established. The IENF density in paw skin from transplanted mice had increased significantly at the end of the experiment (5-6 weeks after transplantation) compared to *Ins2^{+/Akita}* mice that had not received an islet transplant. The IENF density in transplanted mice was indistinguishable from that in healthy wildtype mice (Fig. 7B).

DISCUSSION

Here, we present a detailed characterization of sensory neuropathy in the *Ins2^{+/Akita}* mouse, and demonstrate that diabetes leads to an impaired mechanical and thermal (hot and cold) nociception, which is associated with a marked loss of IENFs. We noted a rapid loss of mechanical nociception at the onset of diabetes, which was followed by a reduced sensitivity to noxious cold and heat 2-3 weeks later. In contrast, we did not observe an altered sensitivity to stimulation with von Frey filaments. We used manual stimulation with calibrated von Frey filaments according to Chaplan's up-down method (17), rather than the widely used automated von Frey assay (5), which employs stimuli of higher force intensity and generates higher paw withdrawal thresholds. Our behavioral and electrophysiological studies suggest that mechano-nociceptors are particularly sensitive to diabetes, whereas low-threshold A-fibers are functionally more resilient. Intriguingly, the loss of mechanical nociception appears to be a dynamic process, with rapid onset after the establishment of hyperglycemia, and a similarly rapid recovery following islet transplantation. In addition, the recovery of female *Ins2^{+/Akita}* mice from hyperglycemia was accompanied by a normalized sensitivity in the paw-pressure test. The distinct behavioral profiles observed using different test modalities underscores the value of employing a comprehensive behavioral testing strategy.

Mechanosensation

Patients with diabetic neuropathy commonly report numbness, spontaneous pain and dysesthesias (34), but loss of thermal (cold and heat detection) and mechanical (mechanical and vibration detection) sensation are the dominant sensory symptoms in patients with mild, severe or no pain (3,35). Hypersensitivity to thermal or mechanical stimulation

(evoked pain) can thus not be viewed as translational measures of spontaneous pain or painful diabetic neuropathy. Importantly, we only observed a reduced responsiveness of mechanosensitive and thermosensitive fibers here, in good agreement with an earlier skin-nerve investigation of mice made diabetic by STZ treatment (36).

Our electrophysiological studies demonstrate that *Ins2^{+/-Akita}* AM and, to a lesser extent, CM nociceptors failed to sustain a high action potential discharge rate in response to intense mechanical stimulation. The force activation threshold of *Ins2^{+/-Akita}* AM fibres, but not CM fibers, was increased somewhat compared to fibers from wildtype mice, whereas C-fibers exhibited a degree of conduction slowing. Together, these results suggest that neuronal excitability and conduction, rather than transduction of mechanical and thermal stimuli, are primarily affected by diabetes in *Ins2^{+/-Akita}* mice. Our results are consistent with the loss of mechanical nociception observed in mice *in vivo* and clinically in patients (1,37,38).

Earlier investigations of STZ induced diabetic neuropathy in mice, demonstrated a reduced mechanical sensitivity of RA fibers, and a more pronounced loss of CM nociceptor activity than observed here in *Ins2^{+/-Akita}* mice (36). It is possible that the longer interval between consecutive mechanical challenges used here may have allowed a fuller recovery of CM fiber activity. Other possible reasons for differences between the two studies include the age of diabetes onset (which is very early in *Ins2^{+/-Akita}*), duration of diabetes, and the possibility that STZ affects cells outside the pancreatic islets (39–42).

Thermal nociception

Diabetic *Ins2^{+/-Akita}* mice displayed an impaired sensitivity to noxious heat and cold *in vivo* and *in vitro*. Studies of temperature sensitive CM fibers (CMHs and CMCs) in isolated skin-nerve preparations from *Ins2^{+/-Akita}* mice, demonstrated a markedly reduced responsiveness

to cold, but not to heat. DRG neurons from *Ins2^{+/Akita}* mice showed a markedly reduced heat responsiveness compared to neurons from wildtype mice, but an unchanged cold sensitivity. The capsaicin receptor TRPV1 is the principal heat transducer in DRG neurons, although other ion channels have been proposed to contribute to transduction of noxious heat, e.g. during inflammation or in response to very high temperatures (43–46). A high concentration of the TRPV1 agonist capsaicin evoked $[Ca^{2+}]_i$ -responses in equal proportions of wildtype and *Ins2^{+/Akita}* DRG neurons, suggesting that an altered expression of TRPV1 is unlikely to explain the reduced heat sensitivity in *Ins2^{+/Akita}*. It is possible that a reduced activity produced by e.g. glycation (47) or altered phosphorylation of TRPV1 may contribute to the reduced sensitivity (48). It is likely that heat evoked $[Ca^{2+}]_i$ -responses are mediated in part by voltage gated Ca^{2+} -channels, following an initial TRPV1 mediated depolarization. An altered activity of voltage gated channels or differences in membrane potential that influences calcium entry via voltage-gated calcium channels, may thus be responsible for the reduced heat sensitivity observed in DRG neurons isolated from *Ins2^{+/Akita}* mice. The reduced heat responsiveness of isolated DRG neurons, but largely unchanged activity of CMH fibers, may indicate that mechano-insensitive heat nociceptors are affected by diabetes.

In contrast to the reduced heat responsiveness of *Ins2^{+/Akita}* DRG neurons, we did not detect any deficits in the neuronal response to cold ramps. We used a modest cooling rate in our experiments, and different rates of cooling are known to stimulate different sensory neuron populations (49,50). It is therefore possible that a sub-population of cold-sensitive *Ins2^{+/Akita}* DRG neurons with altered properties may have been overlooked.

Nociceptive AM and CM fibers, as well as mechanically insensitive thermoreceptors terminate as free nerve endings in the epidermal layer of the skin (51,52). A reduced density of IENFs may thus have contributed to the impaired thermal and mechanical nociceptive function *in vivo*.

Islet transplantation

Transplantation of pancreatic islets isolated from healthy wildtype mice, progressively improved blood glucose and achieved normoglycemia after about three weeks. In contrast, the behavioral sensitivity to noxious mechanical and cold stimulation was restored to the wildtype level by the time of first behavioral test (2-3 days after transplantation). This rapid recovery of sensory function, may indicate that hyperglycemia is not directly responsible for maintaining the impaired nociception. One possible explanation for the rapid restoration of nociceptive function is that insulin itself may modulate sensory neuron function and act as a neurotrophic factor (reviewed in (53)). A rapid neurotrophic or sensitizing effect of insulin on sensory neurons following transplantation, is also consistent with the observation that the insulin signal transduction machinery is intact or even upregulated in Zucker diabetic fatty rats with well-established neuropathy (54). Furthermore, local intraplantar administration of insulin in diabetic mice rapidly (within days) increased the density of IENFs, a time course that is consistent with that observed here for recovery of behavioral sensitivity *in vivo* following islet transplantation (55). In our experiments on isolated DRG neurons, we did not match the insulin concentrations to the levels that the DRG neurons would experience *in vivo*. The observed differences between wildtype and Akita neurons can thus not be explained by any differences in the insulin concentrations in the cell culture medium. Importantly, this also means that the compromised heat sensitivity of *Ins2*^{+/Akita}

neurons, which are in line with our behavioral observations *in vivo* and electrophysiological observations *in vitro*, are due to diabetes, not simply due to differences in insulin signaling after isolation of the neurons. It is likely that sensory neurons exhibit heterogeneous insulin signaling mechanisms, since the expression pattern of the insulin receptor, IRS1 and IRS2 isn't uniform across DRG neurons (56). The concentration of insulin present in the medium here (~4pM) is below the concentrations required to exert trophic effects on isolated sensory neurons (23).

In conclusion, diabetes caused by *Ins2*^{C96Y} is associated with impaired nociception, loss of IENFs, a reduced sensory neuronal heat sensitivity and a reduced action potential discharge rate in mechanosensitive nociceptive afferent fibers *in vitro*. Functional and structural improvement from established diabetic neuropathy was previously reported from mice that recovered spontaneously from STZ-evoked diabetes (57). Our results highlight the importance of distinguishing sensory abnormalities from the spontaneous pain that may be caused by diabetic neuropathy in patients. Islet transplantation restored IENF density (assessed at the end of the experiment, 5-6 weeks after transplantation). Remarkably, islet transplantation restored nociceptive function before normoglycemia was established, indicating that lack of insulin, rather than hyperglycemia per se, is responsible for the impaired nociception in diabetic mice.

Ins2^{+/*Akita*}, and other strains carrying *Ins2* mutations (58), are convenient and attractive models of type 1 diabetes. Here we show that diabetic neuropathy in the *Ins2*^{+/*Akita*} mouse is characterized by a loss of evoked sensory responses, consistent with the sensory profile most commonly observed in patients with painful or painless neuropathy (3). Studies of experimental models which rely on disease relevant mechanisms and faithfully reproduce

the clinical condition, such as the *Ins2^{+/Akita}* mouse, are likely to generate conclusions of translational predictive validity. *Ins2^{+/Akita}* appears to have an advantage over several other commonly used rodent models of diabetic sensory neuropathy that are associated with mechanical hypersensitivity. The hypersensitivity seen in the latter models contrasts with clinical experience in humans where reduced tactile sensitivity is used to detect the onset of diabetic neuropathy. Although patients with painful diabetic neuropathy may display a more marked loss of sensation than those with painless neuropathy, sensory loss is the primary symptom of both groups (3,35,38). Sensory testing of diabetic rodents is thus appropriate as a sensitive experimental measure of sensory neuropathy, but not as a translational measure of spontaneous pain and dysesthesias.

Acknowledgements

N.V., F.G., C.G., A.A. and A.J.K., performed and analyzed experiments. All authors contributed to experimental design and manuscript preparation. D.A.A. is the guarantor of this study and had full access to all the data in the study and takes responsibility for the integrity of the data and the accuracy of the data analysis. This study was supported by the Diabetes UK Alec and Beryl Warren Award to D.A.A., S.B. and A.J.K. (BDA 13/0004649). F.G. was supported by the Johannes und Frieda Marohn-Stiftung. The authors declare no conflict of interest.

FIGURE LEGENDS

Figure 1. Diabetes and nociception in *Ins2^{+/-Akita}* mice. Blood glucose (A) and body weight (B) was monitored weekly in male and female *Ins2^{+/-Akita}* and wildtype littermates. Mechanical nociception was monitored using the paw-pressure test (C) and punctate stimulation with von Frey filaments (D). Thermal nociception was examined using cold (10 °C) and hot (50 °C) plate tests. * $P < 0.05$, ** $P < 0.01$ and *** $P < 0.001$, compared to wildtype mice of the same sex, ANOVA followed by Tukey's. $N = 3-20$ (3 for some measurements at 3-4 and 18 < weeks of age).

Figure 2. Diabetes has a limited impact on low threshold mechanoreceptors. The number of action potentials elicited per second by a 15 s force step in skin-nerve preparations from 20 weeks old male WT and *Ins2^{+/-Akita}* mice is shown for RA, SA and D-hair fibers. (A) RA and (E) D-hair fibers from *Ins2^{+/-Akita}* and wildtype littermates responded similarly in response to all forces. The temporal response pattern to sustained stimuli was indistinguishable between wildtype and *Ins2^{+/-Akita}* RA (B) and D-hair (F) fibers, with high rates of action potentials at the force onset and offset. The mean response to 0.5 g constant force is shown. (C) Diabetic SA fibers responded significantly less to the lowest force of 0.5g ($p = 0.01$, Mann-Whitney *U*-test). (D) Diabetic SA fibers showed a reduced firing rate after the first second to a 0.5g sustained force. ** $p < 0.01$, compared to SA fibers from wildtype mice, Mann-Whitney *U*-test.

Figure 3. A δ mechano-nociceptors are impaired in diabetic *Ins2^{+/-Akita}* mice. (A) *Ins2^{+/-Akita}* AM fibers displayed a reduced rate of action potential discharge in response to 15s applications of 15g and 20g force, compared to wildtype fibers ($p = 0.008$ for 15g, $p = 0.0012$ for 20g, Mann-Whitney *U*-test). (B) *Ins2^{+/-Akita}* AM fibers display a reduced rate of firing in

response to application of 20g force, with a particularly marked reduction during the first few seconds of the stimulus. (C) WT AM fibers attained significantly higher maximal firing rates in response to applications of both 15 and 20g ($p=0.002$ for 15g and $p=0.005$ for 20g, Mann-Whitney *U*-test) compared to diabetic AM fibers. (D) Example traces of *Ins2*^{+/Akita} and wildtype AM fibers demonstrating the markedly reduced response rate in diabetic AM fibers. (E) *Ins2*^{+/Akita} and wildtype AM fibers responses evoked by increasing force ramps. (F) The temporal pattern of impulse discharge rates evoked by 20g force ramps in *Ins2*^{+/Akita} and wildtype AM fibers. * $p<0.05$; ** $p<0.01$, compared to wildtype, Mann-Whitney *U*-test. All fibers were recorded in preparations from 20 weeks old male mice.

Figure 4. C mechano-nociceptors are impaired in diabetic *Ins2*^{+/Akita} mice. The rate of action potential discharge evoked by 15s force steps (A), and the mean temporal discharge pattern produced by 20g steps (B) in *Ins2*^{+/Akita} and wildtype CM fibers are shown. (C) Application of force ramp stimuli evoked a significantly reduced rate of impulse discharge in *Ins2*^{+/Akita} compared to WT CM fibers at 20g, with a pattern of reduced response rates at lower ramp forces ($p=0.035$, Mann-Whitney *U*-test). (D) The mean firing patterns evoked by stimulation of *Ins2*^{+/Akita} and WT CM fibers with 20g ramps, show that diabetic CM fibers respond with reduced discharge rates throughout the stimulus, particularly in response to the peak force at the end of the challenge. (E) Typical traces of the response of *Ins2*^{+/Akita} and WT CM fibers illustrate that diabetic CM fibers produce fewer action potentials in response to application of 20g force ramps. * $p<0.05$; ** $p<0.01$, compared to wildtype, Mann-Whitney *U*-test. All fibers were recorded in preparations from 20 weeks old male mice.

Figure 5. Temperature evoked responses in C-mechano nociceptors. Distribution of temperature thresholds and the temperature change required to elicit cold (**A** and **B**) and heat activation (**F** and **G**) in *Ins2^{+/-Akita}* and wildtype C-mechano nociceptors is shown. The number of cold evoked action potentials was significantly reduced in CM nociceptors from *Ins2^{+/-Akita}* mice compared to wildtype mice as shown by the average response to a 60 second cold ramp (**C**) and their response pattern (**D**). An overall reduction in heat evoked action potentials from *Ins2^{+/-Akita}* mice was observed compared to wildtype mice (**H and I**), but the difference did not reach statistical significance. (**E and J**) Example traces of a wildtype and diabetic CM nociceptors responding to cold and heat, respectively is shown. * $P < 0.05$, compared to wildtype, Mann-Whitney *U*-test, the numbers of studied fibers in the different categories are indicated in panels D and I. All fibers were recorded in preparations from 20 weeks old male mice.

Figure 6. Temperature evoked responses in DRG neurons. (**A**) DRG neurons loaded with Fura-2 were challenged with cold and heat followed by the TRPM8 agonist icilin (1 μ M), the TRPV1 agonist capsaicin (1 μ M) and KCl (50 mM). The black trace is an example of a typical icilin- and cold-sensitive neuron. This neuron exhibits an off-response after the heat ramp, when the temperature is returned to ~ 30 °C. The red trace is an example of a heat- and capsaicin-sensitive neuron. (**B**) Neurons that responded to a temperature ramp with a discontinuous rate of $[Ca^{2+}]_i$ -increase were considered heat/cold sensitive and included in the analysis. Distribution of temperature thresholds for heat activation (**C**) and cold activation (**E**) in *Ins2^{+/-Akita}* and wildtype neurons. (**D**) Heat evoked $[Ca^{2+}]_i$ -response amplitudes were reduced in neurons from *Ins2^{+/-Akita}* mice compared to wildtype mice, whereas the amplitude of cold responses were unchanged (**F**). * $P < 0.05$, *** $P < 0.001$, unpaired t-test. DRG neurons were isolated from male mice of 12 or 20 weeks of age.

Figure 7. Recovery from sensory neuropathy following islet transplantation. (A)

Intraepidermal nerve fibers (IENFs) were visualized by immunostaining for PGP9.5. The scalebar is 20 μ m. **(B)** The IENF density was significantly reduced in skin sections from male 20 weeks old *Ins2^{+/-}/Akita* mice compared to age-matched wildtype littermates. Male diabetic *Ins2^{+/-}/Akita* mice were transplanted at an age of 14-20 weeks. Following islet transplantation (5-6 weeks), the IENF density recovered to the level seen in healthy wildtype mice. **(C)** Blood glucose concentration was progressively restored following islet transplantation, reaching normoglycemic levels after 2-3 weeks. **(D)** The sensitivity to noxious mechanical (paw-pressure test) and **(E)** cold (cold-plate) stimulation rapidly increased to wildtype level following islet transplantation (compare to wildtype in Fig. 1**C**, **E**). Individual data points from each of n=5 transplanted mice are shown in C-E. The areas shaded in grey **(C-E)** indicate the level in male wildtype littermates (mean \pm SD). Data in B are the individual raw values and the box indicates median with interquartile range of n=5-7 mice. *P<0.05, **P<0.01, ***P<0.001, ANOVA followed by Tukey's (compared to *Ins2^{+/-}/Akita* panel B) or Dunnett's (compared to pre-transplantation, panels **C-E**) post-hoc test.

Table 1. Sensory nerve fiber conduction velocity and mechanical thresholds in male 20 weeks old WT and diabetic *Ins2^{+/-Akita}* mice

Values are mean ± SEM (n), P values from Mann-Whitney *U*-test.

Fiber type	WT conduction velocity (m/s)	<i>Ins2^{+/-Akita}</i> conduction velocity (m/s)	P values	WT mechanical threshold (g)	<i>Ins2^{+/-Akita}</i> mechanical threshold (g)	P values
<i>Aβ rapidly adapting</i>	14.3 ± 1.1, (20)	13.4 ± 0.7, (10)	0.71	0.5 ± 0.2, (14)	0.7 ± 0.3, (10)	0.84
<i>Aβ slowly adapting</i>	15.8 ± 1.0, (21)	15.5 ± 2.0, (9)	0.44	0.4 ± 0.1, (12)	0.5 ± 0.1, (9)	0.23
<i>Aδ down hair</i>	7.5 ± 0.3, (16)	6.4 ± 0.6, (11)	0.27	0.2 ± 0.04, (12)	0.2 ± 0.1, (11)	0.34
<i>Aδ A- mechanoreceptor</i>	5.9 ± 0.4, (38)	6.8 ± 1.0, (12)	0.47	2.3 ± 0.3, (32)	2.9 ± 0.3, (12)	0.037
<i>C- mechanoreceptor</i>	0.57 ± 0.02, (45)	0.49 ± 0.02, (28)	0.007	2.3 ± 0.2, (35)	3.0 ± 0.5, (24)	0.9

REFERENCES

1. Boulton AJM. The diabetic foot: from art to science. The 18th Camillo Golgi lecture. *Diabetologia*. 2004 Aug;47(8):1343–53.
2. Fernando ME, Seneviratne RM, Tan YM, Lazzarini PA, Sangla KS, Cunningham M, et al. Intensive versus conventional glycaemic control for treating diabetic foot ulcers. *Cochrane Database Syst Rev*. 2016 Jan 13;(1):CD010764.
3. Themistocleous AC, Ramirez JD, Shillo PR, Lees JG, Selvarajah D, Orengo C, et al. The Pain in Neuropathy Study (PiNS): a cross-sectional observational study determining the somatosensory phenotype of painful and painless diabetic neuropathy. *Pain*. 2016 May;157(5):1132–45.
4. Obrosova IG. Diabetic painful and insensate neuropathy: pathogenesis and potential treatments. *Neurother J Am Soc Exp Neurother*. 2009 Oct;6(4):638–47.
5. Biessels GJ, Bril V, Calcutt NA, Cameron NE, Cotter MA, Dobrowsky R, et al. Phenotyping animal models of diabetic neuropathy: a consensus statement of the diabetic neuropathy study group of the EASD (Neurodiab). *J Peripher Nerv Syst JPNS*. 2014 Jun;19(2):77–87.
6. Farooqi MA, Lovblom LE, Lysy Z, Ostrovski I, Halpern EM, Ngo M, et al. Validation of cooling detection threshold as a marker of sensorimotor polyneuropathy in type 2 diabetes. *J Diabetes Complications*. 2016 Jun;30(4):716–22.
7. Said G. Diabetic neuropathy. *Handb Clin Neurol*. 2013;115:579–89.
8. Lang PM, Schober GM, Rolke R, Wagner S, Hilge R, Offenbächer M, et al. Sensory neuropathy and signs of central sensitization in patients with peripheral arterial disease. *Pain*. 2006 Sep;124(1–2):190–200.
9. Sharma S, Kerry C, Atkins H, Rayman G. The Ipswich Touch Test: a simple and novel method to screen patients with diabetes at home for increased risk of foot ulceration. *Diabet Med J Br Diabet Assoc*. 2014 Sep;31(9):1100–3.
10. Papanas N, Ziegler D. New diagnostic tests for diabetic distal symmetric polyneuropathy. *J Diabetes Complications*. 2011 Feb;25(1):44–51.
11. Callaghan BC, Cheng HT, Stables CL, Smith AL, Feldman EL. Diabetic neuropathy: clinical manifestations and current treatments. *Lancet Neurol*. 2012 Jun;11(6):521–34.
12. Feldman EL, Nave K-A, Jensen TS, Bennett DLH. New Horizons in Diabetic Neuropathy: Mechanisms, Bioenergetics, and Pain. *Neuron*. 2017 Mar 22;93(6):1296–313.
13. Wang J, Takeuchi T, Tanaka S, Kubo SK, Kayo T, Lu D, et al. A mutation in the insulin 2 gene induces diabetes with severe pancreatic beta-cell dysfunction in the Mody mouse. *J Clin Invest*. 1999 Jan;103(1):27–37.
14. Yoshioka M, Kayo T, Ikeda T, Koizumi A. A novel locus, Mody4, distal to D7Mit189 on chromosome 7 determines early-onset NIDDM in nonobese C57BL/6 (Akita) mutant mice. *Diabetes*. 1997 May;46(5):887–94.
15. King AJF. The use of animal models in diabetes research. *Br J Pharmacol*. 2012 Jun;166(3):877–94.

16. Schmidt RE, Green KG, Snipes LL, Feng D. Neuritic dystrophy and neuronopathy in Akita (Ins2(Akita)) diabetic mouse sympathetic ganglia. *Exp Neurol*. 2009 Mar;216(1):207–18.
17. Chaplan SR, Bach FW, Pogrel JW, Chung JM, Yaksh TL. Quantitative assessment of tactile allodynia in the rat paw. *J Neurosci Methods*. 1994 Jul;53(1):55–63.
18. Gentry C, Stoakley N, Andersson DA, Bevan S. The roles of iPLA2, TRPM8 and TRPA1 in chemically induced cold hypersensitivity. *Mol Pain*. 2010 Jan 21;6:4.
19. Andersson DA, Gentry C, Moss S, Bevan S. Clioquinol and pyrithione activate TRPA1 by increasing intracellular Zn²⁺. *Proc Natl Acad Sci U S A*. 2009 May 19;106(20):8374–9.
20. Koltzenburg M, Stucky CL, Lewin GR. Receptive properties of mouse sensory neurons innervating hairy skin. *J Neurophysiol*. 1997 Oct;78(4):1841–50.
21. De Col R, Messlinger K, Carr RW. Repetitive activity slows axonal conduction velocity and concomitantly increases mechanical activation threshold in single axons of the rat cranial dura. *J Physiol*. 2012 Feb 15;590(4):725–36.
22. Bevan S, Winter J. Nerve growth factor (NGF) differentially regulates the chemosensitivity of adult rat cultured sensory neurons. *J Neurosci Off J Soc Neurosci*. 1995 Jul;15(7 Pt 1):4918–26.
23. Fernyhough P, Willars GB, Lindsay RM, Tomlinson DR. Insulin and insulin-like growth factor I enhance regeneration in cultured adult rat sensory neurones. *Brain Res*. 1993 Apr 2;607(1–2):117–24.
24. Kennedy WR, Wendelschafer-Crabb G, Johnson T. Quantitation of epidermal nerves in diabetic neuropathy. *Neurology*. 1996 Oct;47(4):1042–8.
25. Lauria G, Cornblath DR, Johansson O, McArthur JC, Mellgren SI, Nolano M, et al. EFNS guidelines on the use of skin biopsy in the diagnosis of peripheral neuropathy. *Eur J Neurol*. 2005 Oct;12(10):747–58.
26. Jolivald CG, Frizzi KE, Guernsey L, Marquez A, Ochoa J, Rodriguez M, et al. Peripheral Neuropathy in Mouse Models of Diabetes. *Curr Protoc Mouse Biol*. 2016 Sep 1;6(3):223–55.
27. Obrosova IG, Illytska O, Lyzogubov VV, Pavlov IA, Mashtalir N, Nadler JL, et al. High-fat diet induced neuropathy of pre-diabetes and obesity: effects of “healthy” diet and aldose reductase inhibition. *Diabetes*. 2007 Oct;56(10):2598–608.
28. Kerby A, Bohman S, Westberg H, Jones P, King A. Immunoisolation of islets in high guluronic acid barium-alginate microcapsules does not improve graft outcome at the subcutaneous site. *Artif Organs*. 2012 Jun;36(6):564–70.
29. Adriaensen H, Gybels J, Handwerker HO, Hees JV. Response properties of thin myelinated (A-delta) fibers in human skin nerves. *J Neurophysiol*. 1983 Jan 1;49(1):111–22.
30. Torebjörk HE. Afferent C units responding to mechanical, thermal and chemical stimuli in human non-glabrous skin. *Acta Physiol Scand*. 1974 Nov;92(3):374–90.
31. Zochodne DW, Ho LT. The influence of indomethacin and guanethidine on experimental streptozotocin diabetic neuropathy. *Can J Neurol Sci J Can Sci Neurol*. 1992 Nov;19(4):433–41.
32. Johnson MS, Ryals JM, Wright DE. Early loss of peptidergic intraepidermal nerve fibers in an STZ-induced mouse model of insensate diabetic neuropathy. *Pain*. 2008 Nov 15;140(1):35–47.

33. Sumner CJ, Sheth S, Griffin JW, Cornblath DR, Polydefkis M. The spectrum of neuropathy in diabetes and impaired glucose tolerance. *Neurology*. 2003 Jan 14;60(1):108–11.
34. Baron R, Tölle TR, Gockel U, Brosz M, Freynhagen R. A cross-sectional cohort survey in 2100 patients with painful diabetic neuropathy and postherpetic neuralgia: Differences in demographic data and sensory symptoms. *Pain*. 2009 Nov;146(1–2):34–40.
35. Scherens A, Maier C, Haussleiter IS, Schwenkreis P, Vlckova-Moravcova E, Baron R, et al. Painful or painless lower limb dysesthesias are highly predictive of peripheral neuropathy: comparison of different diagnostic modalities. *Eur J Pain Lond Engl*. 2009 Aug;13(7):711–8.
36. Lennertz RC, Medler KA, Bain JL, Wright DE, Stucky CL. Impaired sensory nerve function and axon morphology in mice with diabetic neuropathy. *J Neurophysiol*. 2011 Aug;106(2):905–14.
37. Maier C, Baron R, Tölle TR, Binder A, Birbaumer N, Birklein F, et al. Quantitative sensory testing in the German Research Network on Neuropathic Pain (DFNS): somatosensory abnormalities in 1236 patients with different neuropathic pain syndromes. *Pain*. 2010 Sep;150(3):439–50.
38. Ørstavik K, Namer B, Schmidt R, Schmelz M, Hilliges M, Weidner C, et al. Abnormal Function of C-Fibers in Patients with Diabetic Neuropathy. *J Neurosci*. 2006 Nov 1;26(44):11287–94.
39. Hidmark AS, Nawroth PP, Fleming T. STZ causes depletion of immune cells in sciatic nerve and dorsal root ganglion in experimental diabetes. *J Neuroimmunol*. 2017 May 15;306:76–82.
40. Andersson DA, Filipović MR, Gentry C, Eberhardt M, Vastani N, Leffler A, et al. Streptozotocin Stimulates the Ion Channel TRPA1 Directly: INVOLVEMENT OF PEROXYNITRITE. *J Biol Chem*. 2015 Jun 12;290(24):15185–96.
41. Cunha JM, Funez MI, Cunha FQ, Parada CA, Ferreira SH. Streptozotocin-induced mechanical hypernociception is not dependent on hyperglycemia. *Braz J Med Biol Res Rev Bras Pesqui Medicas E Biol*. 2009 Feb;42(2):197–206.
42. Bishnoi M, Bosgraaf CA, Abooj M, Zhong L, Premkumar LS. Streptozotocin-induced early thermal hyperalgesia is independent of glycemic state of rats: role of transient receptor potential vanilloid 1 (TRPV1) and inflammatory mediators. *Mol Pain*. 2011 Jul 27;7:52.
43. Tominaga M, Caterina MJ, Malmberg AB, Rosen TA, Gilbert H, Skinner K, et al. The cloned capsaicin receptor integrates multiple pain-producing stimuli. *Neuron*. 1998 Sep;21(3):531–43.
44. Caterina MJ, Schumacher MA, Tominaga M, Rosen TA, Levine JD, Julius D. The capsaicin receptor: a heat-activated ion channel in the pain pathway. *Nature*. 1997 Oct 23;389(6653):816–24.
45. Cho H, Yang YD, Lee J, Lee B, Kim T, Jang Y, et al. The calcium-activated chloride channel anoctamin 1 acts as a heat sensor in nociceptive neurons. *Nat Neurosci*. 2012 Jul;15(7):1015–21.
46. Vriens J, Owsianik G, Hofmann T, Philipp SE, Stab J, Chen X, et al. TRPM3 Is a Nociceptor Channel Involved in the Detection of Noxious Heat. *Neuron*. 2011 Dec 5;70(3):482–94.
47. Orestes P, Osuru HP, McIntire WE, Jacus MO, Salajegheh R, Jagodic MM, et al. Reversal of neuropathic pain in diabetes by targeting glycosylation of Ca(V)3.2 T-type calcium channels. *Diabetes*. 2013 Nov;62(11):3828–38.
48. Bevan S, Quallo T, Andersson DA. TRPV1. *Handb Exp Pharmacol*. 2014;222:207–45.

49. Babes A, Zorzon D, Reid G. Two populations of cold-sensitive neurons in rat dorsal root ganglia and their modulation by nerve growth factor. *Eur J Neurosci*. 2004 Nov 1;20(9):2276–82.
50. Babes A, Zorzon D, Reid G. A novel type of cold-sensitive neuron in rat dorsal root ganglia with rapid adaptation to cooling stimuli. *Eur J Neurosci*. 2006 Aug;24(3):691–8.
51. Dhaka A, Earley TJ, Watson J, Patapoutian A. Visualizing Cold Spots: TRPM8-Expressing Sensory Neurons and Their Projections. *J Neurosci*. 2008 Jan 16;28(3):566–75.
52. Iggo A. Cutaneous receptors and their sensory functions. *J Hand Surg Edinb Scotl*. 1984 Feb;9(1):7–10.
53. Grote CW, Wright DE. A Role for Insulin in Diabetic Neuropathy. *Front Neurosci*. 2016;10:581.
54. Brussee V, Cunningham FA, Zochodne DW. Direct insulin signaling of neurons reverses diabetic neuropathy. *Diabetes*. 2004 Jul;53(7):1824–30.
55. Guo G, Kan M, Martinez JA, Zochodne DW. Local insulin and the rapid regrowth of diabetic epidermal axons. *Neurobiol Dis*. 2011 Aug;43(2):414–21.
56. Usoskin D, Furlan A, Islam S, Abdo H, Lönnnerberg P, Lou D, et al. Unbiased classification of sensory neuron types by large-scale single-cell RNA sequencing. *Nat Neurosci*. 2015 Jan;18(1):145–53.
57. Kennedy JM, Zochodne DW. Experimental diabetic neuropathy with spontaneous recovery: is there irreparable damage? *Diabetes*. 2005 Mar;54(3):830–7.
58. Herbach N, Rathkolb B, Kemter E, Pichl L, Klaften M, de Angelis MH, et al. Dominant-negative effects of a novel mutated Ins2 allele causes early-onset diabetes and severe beta-cell loss in Munich Ins2C95S mutant mice. *Diabetes*. 2007 May;56(5):1268–76.

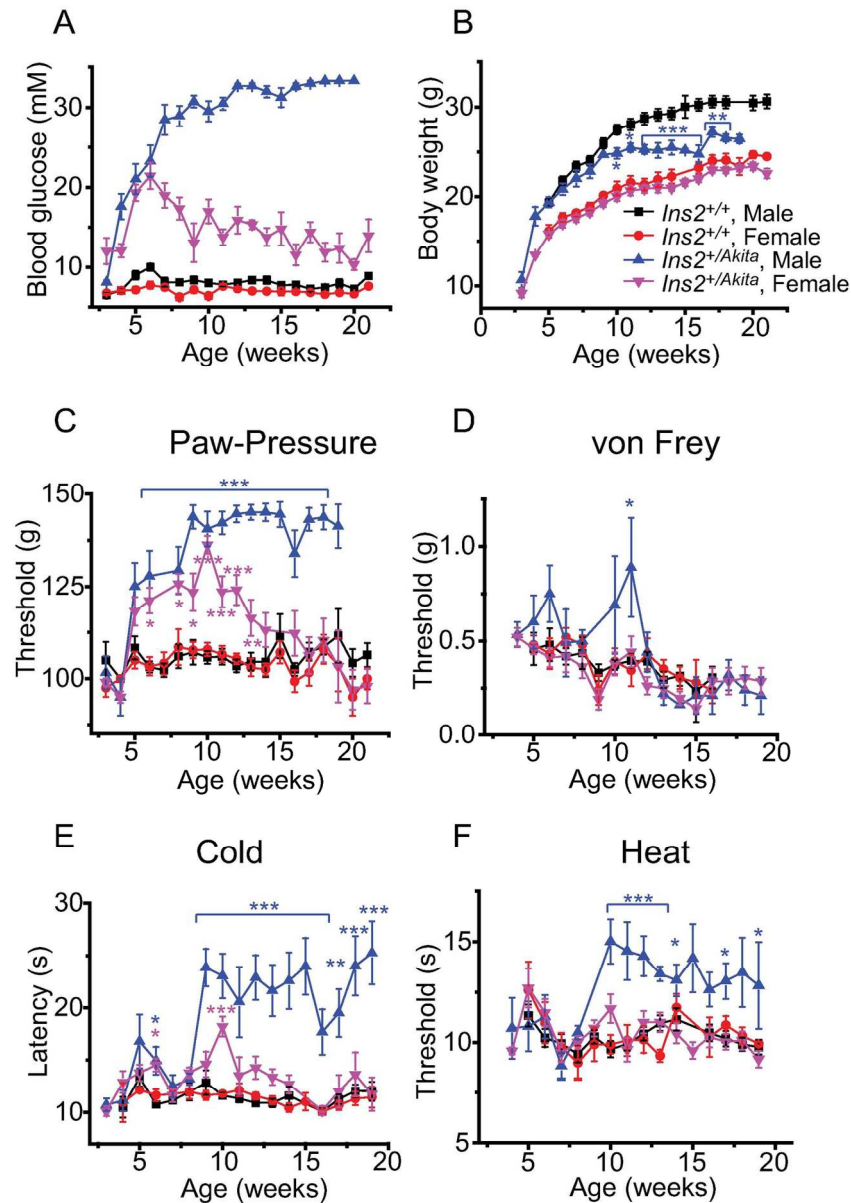


Figure 1. Diabetes and nociception in *Ins2*^{+/Akita} mice. Blood glucose (A) and body weight (B) was monitored weekly in male and female *Ins2*^{+/Akita} and wildtype littermates. Mechanical nociception was monitored using the paw-pressure test (C) and punctate stimulation with von Frey filaments (D). Thermal nociception was examined using cold (10 °C) and hot (50 °C) plate tests. **P*<0.05, ***P*<0.01 and ****P*<0.001, compared to wildtype mice of the same sex, ANOVA followed by Tukey's. *N*=3-20 (3 for some measurements at 3-4 and 18< weeks of age).

127x182mm (300 x 300 DPI)

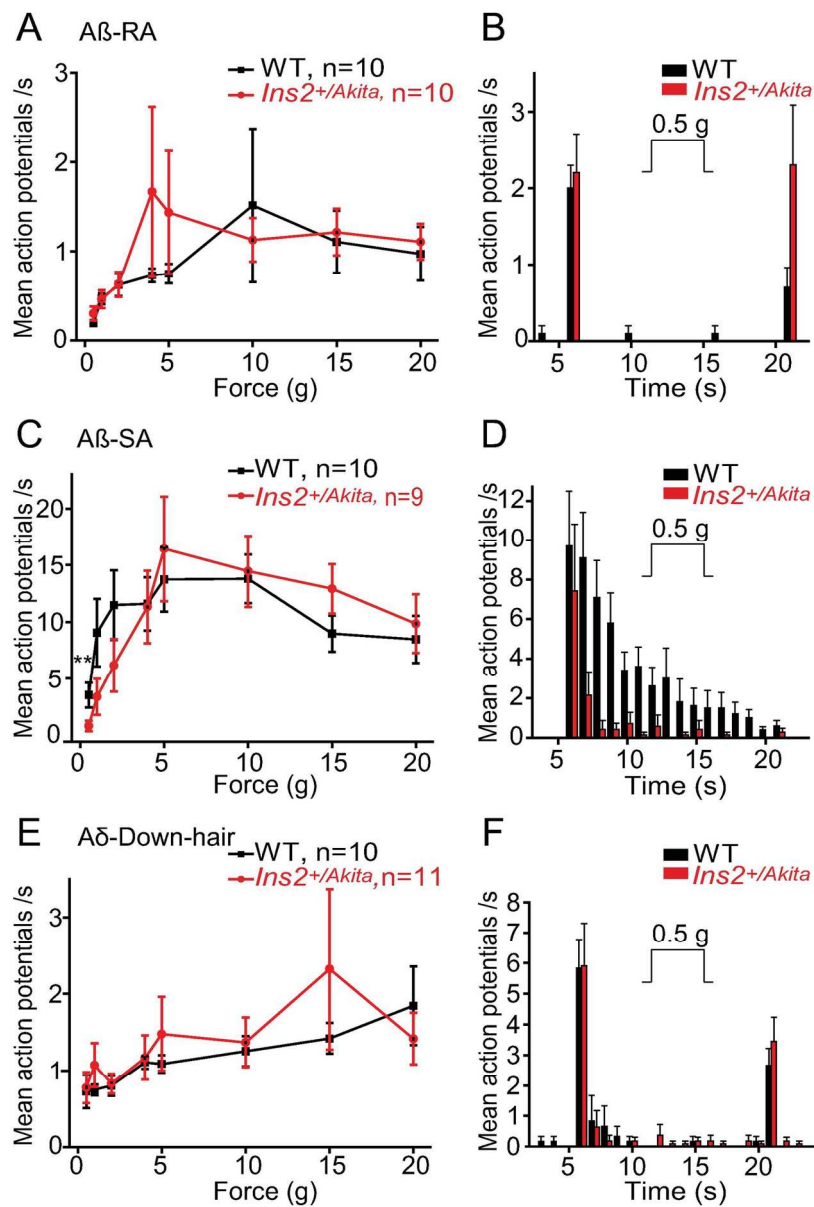


Figure 2. Diabetes has a limited impact on low threshold mechanoreceptors. The number of action potentials elicited per second by a 15 s force step in skin-nerve preparations from 20 weeks old male WT and *Ins2^{+/Akita}* mice is shown for RA, SA and D-hair fibers. (A) RA and (E) D-hair fibers from *Ins2^{+/Akita}* and wildtype littermates responded similarly in response to all forces. The temporal response pattern to sustained stimuli was indistinguishable between wildtype and *Ins2^{+/Akita}* RA (B) and D-hair (F) fibers, with high rates of action potentials at the force onset and offset. The mean response to 0.5 g constant force is shown. (C) Diabetic SA fibers responded significantly less to the lowest force of 0.5g ($p=0.01$, Mann-Whitney U-test). (D) Diabetic SA fibers showed a reduced firing rate after the first second to a 0.5g sustained force. $^{**}p<0.01$, compared to SA fibers from wildtype mice, Mann-Whitney U-test.

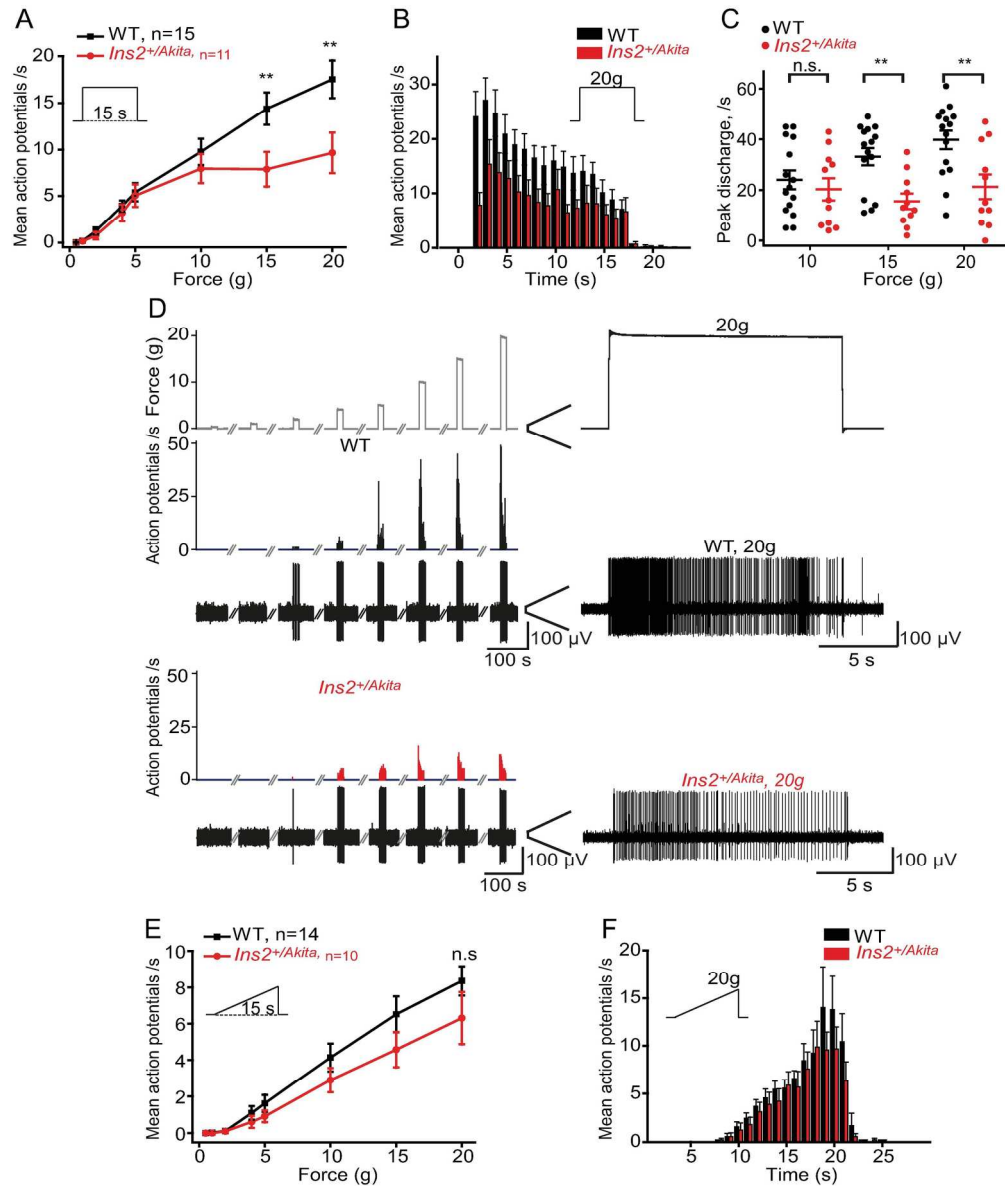


Figure 3. A δ mechanonociceptors are impaired in diabetic *Ins2*^{+/Akita} mice. (A) *Ins2*^{+/Akita} AM fibers displayed a reduced rate of action potential discharge in response to 15s applications of 15g and 20g force, compared to wildtype fibers ($p=0.008$ for 15g, $p=0.0012$ for 20g, Mann-Whitney U-test). (B) *Ins2*^{+/Akita} AM fibers display a reduced rate of firing in response to application of 20g force, with a particularly marked reduction during the first few seconds of the stimulus. (C) WT AM fibers attained significantly higher maximal firing rates in response to applications of both 15 and 20g ($p=0.002$ for 15g and $p=0.005$ for 20g, Mann-Whitney U-test) compared to diabetic AM fibers. (D) Example traces of *Ins2*^{+/Akita} and wildtype AM fibers demonstrating the markedly reduced response rate in diabetic AM fibers. (E) *Ins2*^{+/Akita} and wildtype AM fibers responses evoked by increasing force ramps. (F) The temporal pattern of impulse discharge rates evoked by 20g force ramps in *Ins2*^{+/Akita} and wildtype AM fibers. * $p<0.05$; ** $p<0.01$, compared to wildtype, Mann-Whitney U-test. All fibers were recorded in preparations from 20 weeks old male mice.

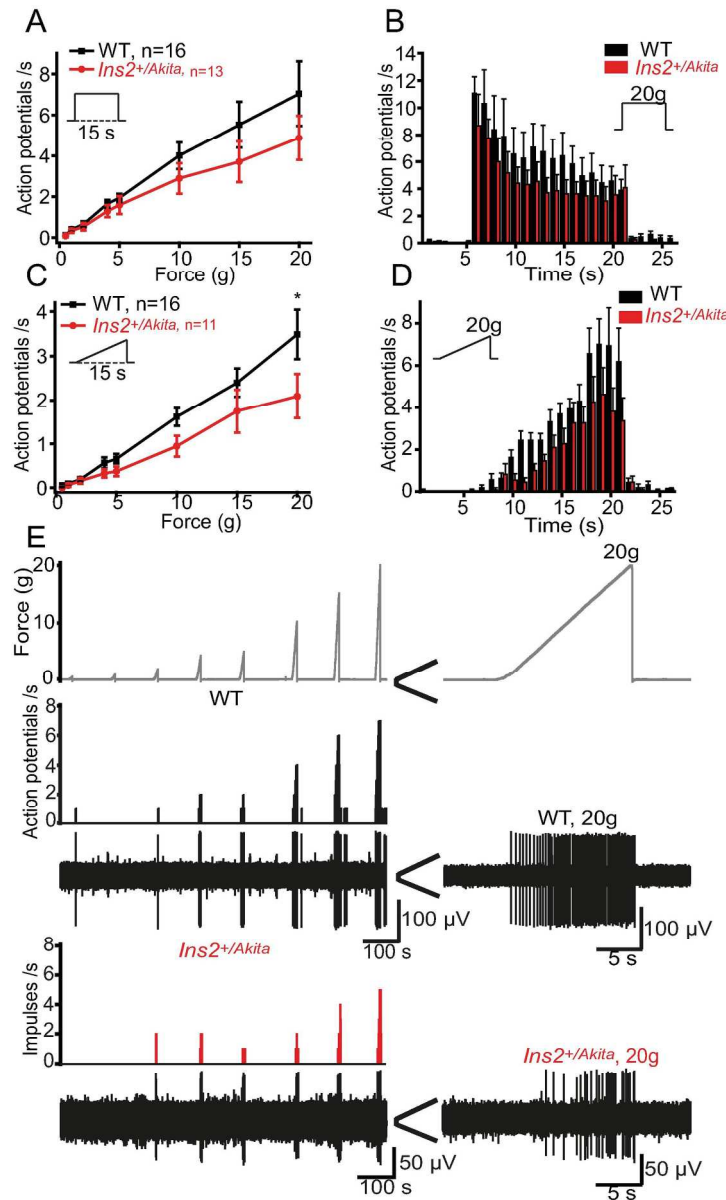


Figure 4. C mechanonociceptors are impaired in diabetic *Ins2+/Akita* mice. The rate of action potential discharge evoked by 15s force steps (A), and the mean temporal discharge pattern produced by 20g steps (B) in *Ins2+/Akita* and wildtype CM fibers are shown. (C) Application of force ramp stimuli evoked a significantly reduced rate of impulse discharge in *Ins2+/Akita* compared to WT CM fibers at 20g, with a pattern of reduced response rates at lower ramp forces ($p=0.035$, Mann-Whitney U-test). (D) The mean firing patterns evoked by stimulation of *Ins2+/Akita* and WT CM fibers with 20g ramps, show that diabetic CM fibers respond with reduced discharge rates throughout the stimulus, particularly in response to the peak force at the end of the challenge. (E) Typical traces of the response of *Ins2+/Akita* and WT CM fibers illustrate that diabetic CM fibers produce fewer action potentials in response to application of 20g force ramps. * $p<0.05$; ** $p<0.01$, compared to wildtype, Mann-Whitney U-test. All fibers were recorded in preparations from 20 weeks old male mice.

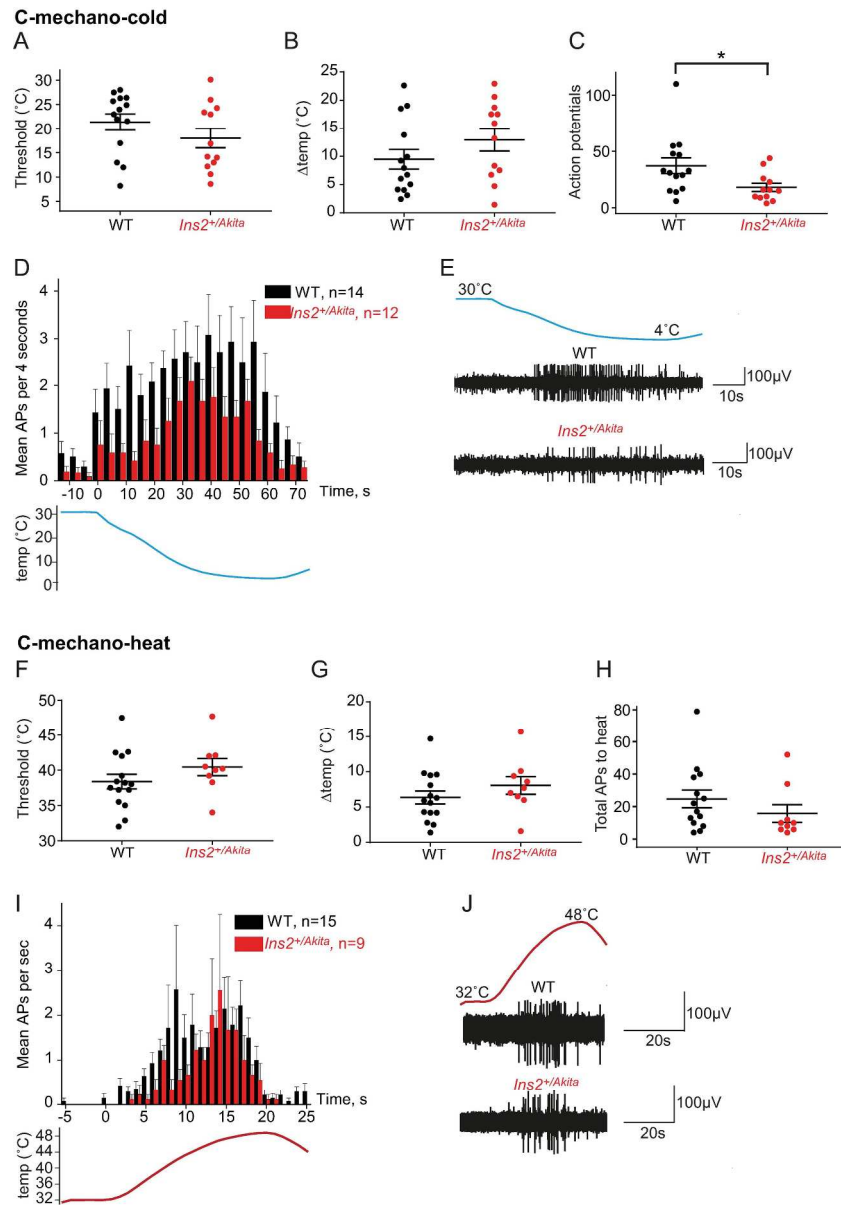


Figure 5. Temperature evoked responses in C-mechano nociceptors. Distribution of temperature thresholds and the temperature change required to elicit cold (A and B) and heat activation (F and G) in *Ins2^{+/Akita}* and wildtype C-mechano nociceptors is shown. The number of cold evoked action potentials was significantly reduced in CM nociceptors from *Ins2^{+/Akita}* mice compared to wildtype mice as shown by the average response to a 60 second cold ramp (C) and their response pattern (D). An overall reduction in heat evoked action potentials from *Ins2^{+/Akita}* mice was observed compared to wildtype mice (H and I), but the difference did not reach statistical significance. (E and J) Example traces of a wildtype and diabetic CM nociceptors responding to cold and heat, respectively is shown. * $P < 0.05$, compared to wildtype, Mann-Whitney U-test, the numbers of studied fibers in the different categories are indicated in panels D and I. All fibers were recorded in preparations from 20 weeks old male mice.

216x311mm (300 x 300 DPI)

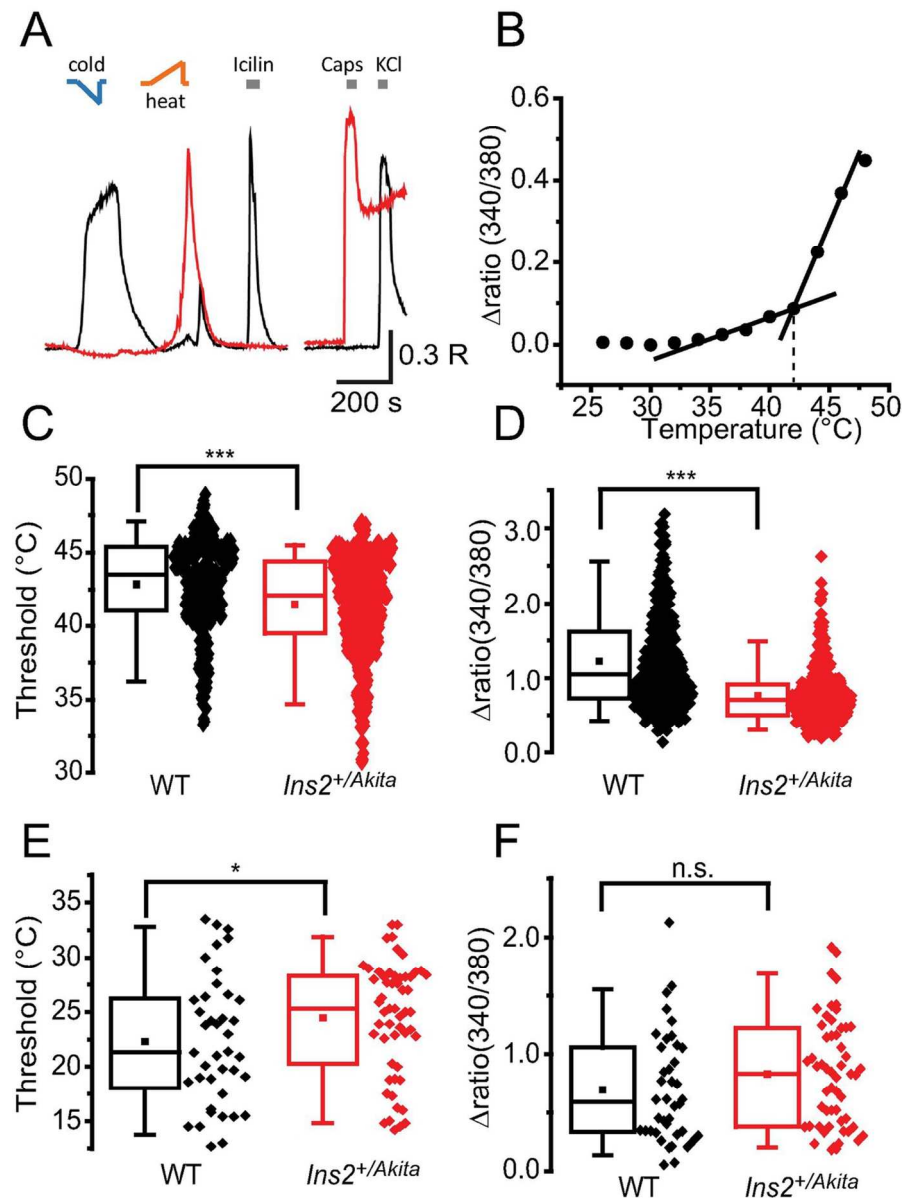


Figure 6. Temperature evoked responses in DRG neurons. (A) DRG neurons loaded with Fura-2 were challenged with cold and heat followed by the TRPM8 agonist icilin (1 μM), the TRPV1 agonist capsaicin (1 μM) and KCl (50 mM). The black trace is an example of a typical icilin- and cold-sensitive neuron. This neuron exhibits an off-response after the heat ramp, when the temperature is returned to $\sim 30^{\circ}\text{C}$. The grey trace is an example of a heat- and capsaicin-sensitive neuron. (B) Neurons that responded to a temperature ramp with a discontinuous rate of $[\text{Ca}^{2+}]_i$ -increase were considered heat/cold sensitive and included in the analysis. Distribution of temperature thresholds for heat activation (C) and cold activation (E) in *Ins2^{+/Akita}* and wildtype neurons. (D) Heat evoked $[\text{Ca}^{2+}]_i$ -response amplitudes were reduced in neurons from *Ins2^{+/Akita}* mice compared to wildtype mice, whereas the amplitude of cold responses were unchanged (F). * $P < 0.05$, *** $P < 0.001$, unpaired t-test. DRG neurons were isolated from male mice of 12 or 20 weeks of age.

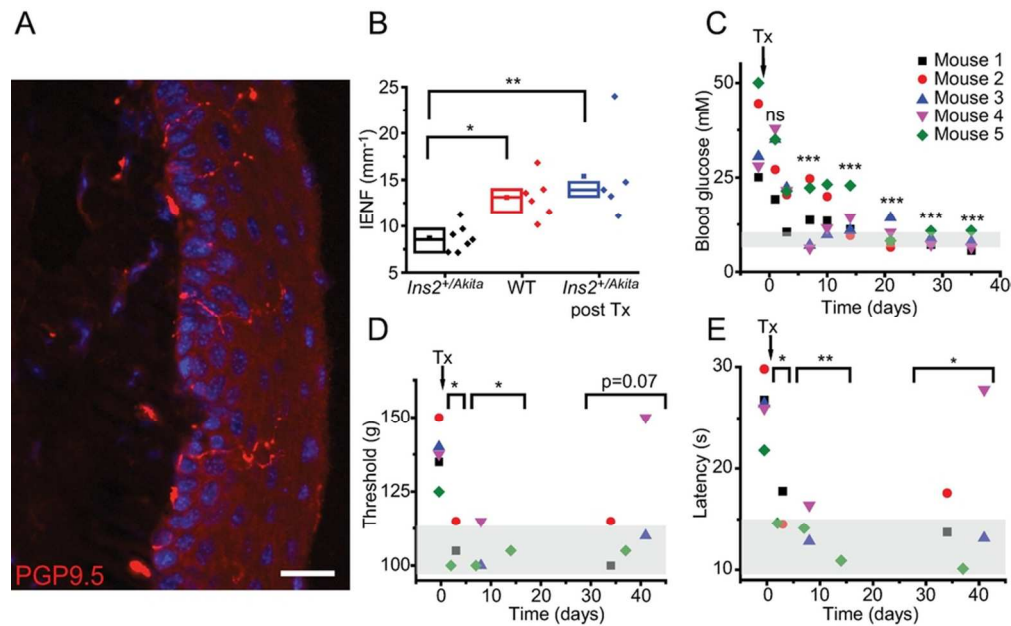


Figure 7. Recovery from sensory neuropathy following islet transplantation. (A) Intraepidermal nerve fibers (IENFs) were visualized by immunostaining for PGP9.5. The scalebar is 20 μ m. (B) The IENF density was significantly reduced in skin sections from male 20 weeks old *Ins2*^{+/Akita} mice compared to age-matched wildtype littermates. Male diabetic *Ins2*^{+/Akita} mice were transplanted at an age of 14-20 weeks. Following islet transplantation (5-6 weeks), the IENF density recovered to the level seen in healthy wildtype mice. (C) Blood glucose concentration was progressively restored following islet transplantation, reaching normoglycemic levels after 2-3 weeks. (D) The sensitivity to noxious mechanical (paw-pressure test) and (E) cold (cold-plate) stimulation rapidly increased to wildtype level following islet transplantation (compare to wildtype in Fig. 1C, E). Individual data points from each of *n*=5 transplanted mice are shown in C-E. The areas shaded in grey (C-E) indicate the level in male wildtype littermates (mean \pm SD). Data in B are the individual raw values and the box indicates median with interquartile range of *n*=5-7 mice. **P*<0.05, ***P*<0.01, ****P*<0.001, ANOVA followed by Tukey's (compared to *Ins2*^{+/Akita} panel B) or Dunnett's (compared to pre-transplantation, panels C-E) post-hoc test.

83x51mm (300 x 300 DPI)